

MAGNETIC KEY TO MICROWORLD

This door and this golden key were
made a long time ago by some skilled
craftsman.

*L.N. Tolstoy "The Golden Key, or the
Adventures of Buratino" [1]*

The atom has long been considered an open book: supposedly all the mysteries of the microworld have already been solved and the structure of atoms and subatomic particles is known [2]. But in recent years, a number of phenomena have been discovered that fundamentally contradict the concepts of the structure of atoms and elementary particles [3]. Thus, a number of anomalies were discovered in the scattering of high-energy protons. High-temperature superconductors have been discovered among ferromagnets, although magnetism has always hindered superconductivity [4]. These surprises in search of scientists are reminiscent of the experiments of Edison, who sorted through thousands of types of wood, before finding the right material for the filament in an incandescent lamp. And the true inventor of the lamp, Lodygin, immediately found a suitable carbon and then a tungsten filament. Similarly, scientists who accidentally discover superconductivity and other properties are usually discouraged, like the carpenter Giuseppe, who discovered the amazing properties of log. Such surprises when searching by the “scientific poke” method arise from ignorance of the structure of atoms and their conglomerates. That is why there are still no fantastic devices, such as levitators, portable reactors, etc. But such knowledge is provided by the ballistic theory (BTR) and the Ritz magnetic model of the atom, which reveals all the secrets of the microworld as a magnetic key [5]. Spectroscopy, which emerged when Newton punched a hole in the shutter and decomposed light into a spectrum, will become the guiding thread in the labyrinth of the atom. So let's begin the journey to the center of the atom, continuing the deciphering of the runes of atomic spectra, begun by Kirchhoff and Bunsen in the same 1860s, when Jules Verne's hero, having deciphered the runes of the ancient alchemist A. Saknussem, undertook a journey to the center of the Earth.

Let us consider the Zeeman effect as a touchstone. Earlier it was shown that the magnetic model of the atom perfectly explains the effect [5]. We recall that the Zeeman effect consists in the splitting of each spectral line into a number of components. But the number, position and intensity of the components often do not match the predictions of quantum theory. Therefore, new models and their refinements are introduced in order to achieve correspondence, and in Ritz's theory everything turns out by itself.

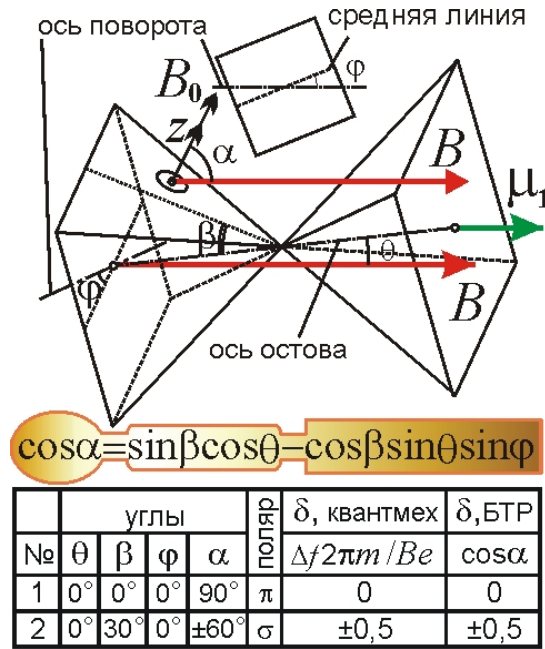


Рис.1. Ключевая формула для угла меж магнитным полем B и нормалью к грани и таблица нормального расщепления.

Fig. 1. Key formula for the angle between magnetic field B and normal to the face and a normal splitting table.

According to Ritz's theory, the Zeeman effect is due to the imposition of an external magnetic field B on the intra-atomic field B_0 of the bipyramidal skeleton of an atom (Fig. 1). Then the electron spinning in the magnetic field of the atom B_0 with a fixed frequency $f_0 = eB_0/2\pi m$ changes the rotation frequency by $f = e(B_0 + B_z)/2\pi m$. The projection of the field $B_z = B\cos\alpha$ onto the normal z to the plane of rotation of the electron can take on a number of values, depending on the orientation of the atom to the external field and on which face the generating electron sits on. Accordingly, instead of one line, a number of lines with close frequencies are generated [5]. Earlier, we discussed the generation of the Lorentz triplet - three lines in the simple Zeeman effect. Even here, quantum theory makes a number of mistakes. Thus, quantum theory predicts that when observing along the magnetic field, only two lines are visible, but in fact, three lines are visible, in accordance with the magnetic model [5], but the radiation of the central line is not polarized, and its intensity is low, since it is generated by electrons on the wall of the core, where the electron can appear with a probability of $1/3$. In addition, for an electron flying in a circular orbit, according to the directional diagram, the radiation intensity in the orbital plane is two times lower than in the transverse one. And when viewed through polarizers that measure circular polarization, the intensity is further reduced. The random movement of electrons from node to node and the corresponding intensities of spectral lines can be calculated by the Monte Carlo method.

And now let us investigate more complex splitting patterns, for example, into the spectrum of sodium, studied in detail by the spectroscopist R. Wood, who was not inferior in terms of mischief and detective searches to a wooden man [6]. The sodium yellow line D_1 is split into 4 components. The fact is that for the type of sodium atoms that generates this line, the cores in an external magnetic field orient the axes not along the field B , but at an angle θ , due to the presence of the core, in addition to its own magnetic moment, the magnetic moment of electrons, and the total moment μ_1 directed at an angle θ to the skeleton axis (Fig. 2). As a result, the pyramidal atomic core in field B rotates around the diagonal of the square base by an angle θ , and the frequencies $f=f_0(1\pm B_1/B_0)$ are generated for electrons sitting on two adjacent side faces, and for electrons on the other two faces $f=f_0(1\pm B_2/B_0)$, where the projections $B_1=B\cos\alpha_1$, $B_2=B\cos\alpha_2$. Then, instead of one, 4 close lines of almost equal intensity arise, since the placement of an electron on all four sides of the skeleton is equally probable, as are the probabilities of pulling a given suit from a deck of cards, often folded in a pyramid, such as the skeleton of an atom. It is easy to find B_1 , B_2 and angles α and θ from the difference in frequencies (Fig. 2). At such angles α , it is clear why the lines corresponding to $\alpha_1=72^\circ$ have a longitudinal field B π -polarization, and $\alpha_2=50^\circ$ - transverse σ -polarization. Because $\alpha_1\neq 90^\circ$, $\alpha_2\neq 0^\circ$ and the core can rotate around B , weak σ and π components can also be observed in the lines.

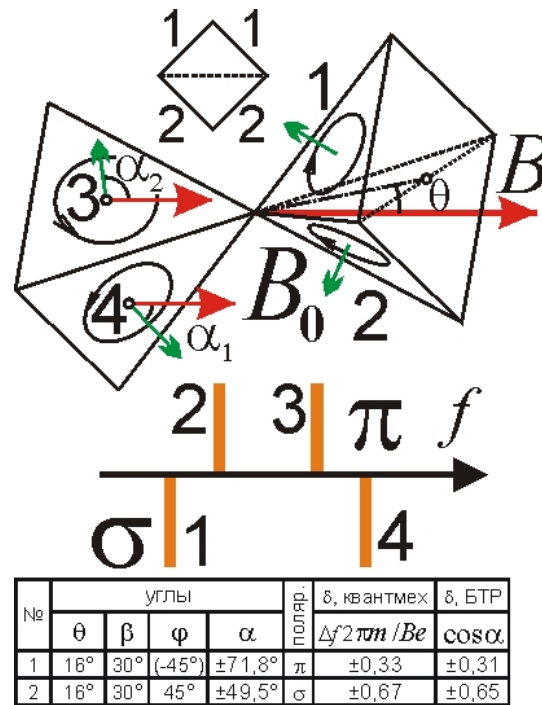


Рис. 2. Схема расщепления D_1 -линии натрия в магнитном поле B на четыре компоненты с указанием поляризаций.

Fig. 2. Scheme of splitting D_1 -line sodium in a magnetic field B by four components with indication of polarization.

Let us estimate strictly the splitting value. The angle between the face and the axis of the bipyramid is $\beta = 30^\circ$ [5], and this axis is rotated at an angle θ to the field B , around the axis of rotation located at the base of one of the pyramids at an angle φ to the midline of the square base (Fig. 1). Then it is easy to find from trigonometry that the angle α between the normal z and the field B is $\cos\alpha = \sin\beta \cdot \cos\theta - \cos\beta \cdot \sin\theta \cdot \sin\varphi$. This golden ratio of five elements gives the key to the atomic pyramid and the calculation of the splitting value $\Delta f = eB \cos\alpha / 2\pi m$, for any rotation of the core in the polar angle θ and azimuthal angle φ . If we assume that the displacements Δf are close to those calculated by quantum mechanics, we obtain for the D_1 line the following angles φ , α and splitting $\delta = \Delta f 2\pi m / eB = \cos\alpha$ (Fig. 2). It is seen that the calculated values of δ do not coincide with the known ones. Indeed, accurate measurements showed deviations from the quantum calculation: the multiplicity (Runge's rule) is slightly violated and the symmetry of the line displacement is violated. This shows the advantages of the classic model. However, it is also imperfect, since it predicts symmetrical displacements. It is just that the calculation did not take into account the magnetic moment of the emitting electron itself, its moment, when added to the moment of the core, depending on the face, gives a slightly different total moment μ_1 . Those, slightly different angles θ correspond to different positions of the electron. Accordingly, the angles α will also slightly change, breaking the symmetry.

Another doublet line, D_2 , splits into 6 components, since the skeleton is already rotated around the midline of the square base of the pyramidal framework through the angle α_2 . Accordingly, on the upper face of the skeleton, the field $B_1 = B \cos\alpha_1$, on the two opposite side faces $B_2 = B \cos\alpha_2$, on the lower face $B_3 = B \cos\alpha_3$. As a result, the brightness of the two middle spectral lines corresponding to B_2 will be twice as high. an electron has twice the probability of being on them than on the top or bottom. The polarizations of the lines are also understandable (Fig. 3). In addition, the intensity depends on the angle α , since the radiation pattern for a radiator in the form of a rotating charge gives maxima in the direction perpendicular to the plane of the charge orbit, and when a given polarization π or σ is released, part of the intensity is lost. For π -polarization, the maximum intensity is achieved at α close to 90° , and for σ - at α close to 0° . From the radiation pattern, averaging over all angles of rotation of the skeleton around the field line \mathbf{B} , it is easy to find the exact value of the line intensity. It can be seen that the displacements found do not quite coincide with the calculated ones using quantum mech. Indeed, accurate measurements show that the line shifts do not quite correspond to quantum theory.

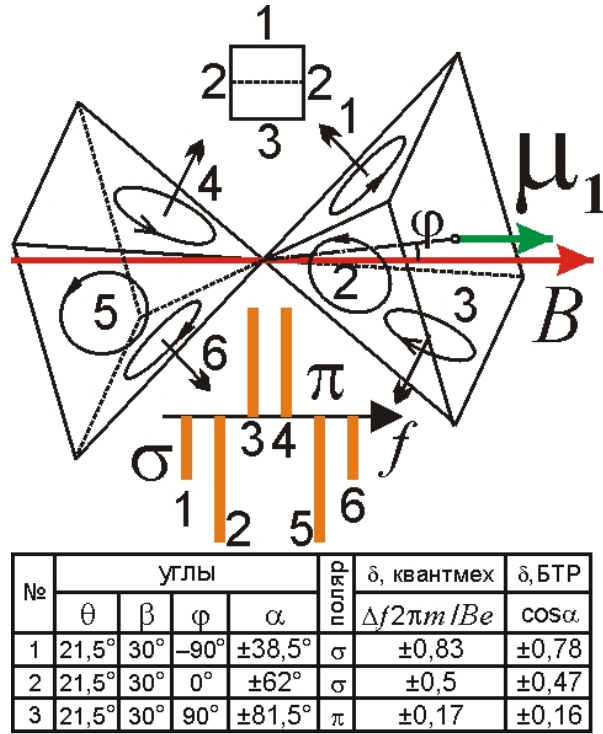


Рис. 3. Схема расщепления D₂-линии натрия в магнитном поле B на шесть компонент с указанием поляризаций.

Fig. 3. Scheme of splitting of the D₂-line sodium in a magnetic field B by six component with indication of polarization.

For other elements, the splitting of the doublet lines into a larger number of components is possible. So, if the atomic core is rotated by a small angle θ_3 relative to a line that does not coincide either with the diagonal of the square base of the core or with the middle line, then the angles to the field B of all four side faces will slightly differ from each other and from the value at $\theta_3 = 0^\circ$. Accordingly, each line of the Lorentz triplet is transformed into four lines corresponding to different faces, or partitions, on which the generating electron is located (Fig. 4). It is this picture of splitting that is observed [7].

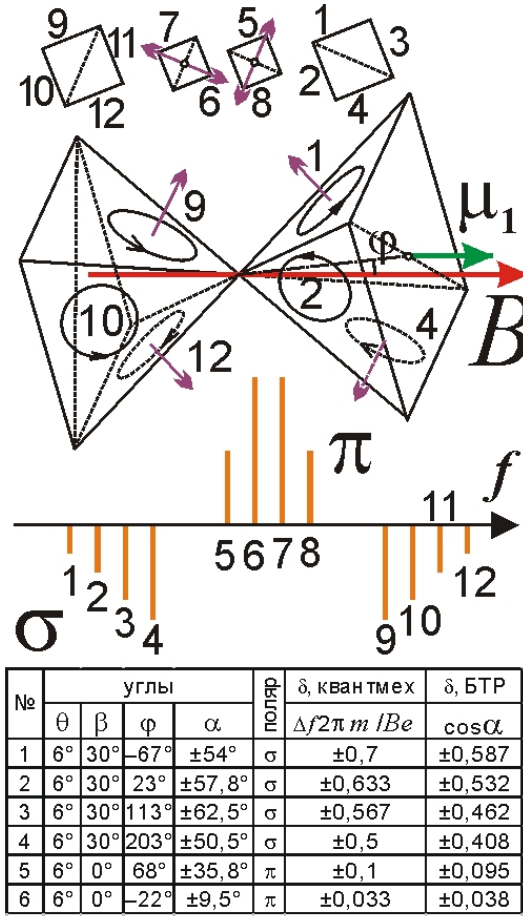


Рис. 4. Схема расщепления линии дублета $^2P_{3/2}$ - $^2D_{5/2}$ в поле B на 12 компонент с указанием поляризаций.

Fig. 4. Line splitting scheme $^2P_{3/2}$ - $^2D_{5/2}$ in field B by 12 components with indication of polarizations.

The components located closer to the original frequency f_0 are polarized along the field (π -polarization), since the plane in which the electrons rotate is almost parallel to the field ($\alpha \approx 90^\circ$). And the components located farther from f_0 have σ -polarization transverse to the field. This is natural in the magnetic model, since the frequency shift $\Delta f = eB \cos \alpha / 2\pi m$, and the smaller the angle α to the field B , the closer the polarization is to transverse σ and the greater the frequency shift Δf . Thus, the magnetic model explains in an elementary way why the polarization is such and not different, which quantum mechanics cannot. In this case, there are no strict boundaries between one and the other polarization, but, starting from a certain angle α , one begins to prevail over the other. This is clearly seen in the Zeeman effect observed from the adsorption spectrum - there are regions in which components with π - and σ -polarization are present at once. And in the spectrum of radiation there are lines at the border, which have both components π - and σ - [7]. This means that the electron

moves in a circle, and we only select the components of this movement and radiation with a polarizer.

In the case of triplets, the atom can already take two positions with respect to the external field: one - when the moment of the core is co-directed with the field B , the second - when the core is inclined at an angle θ to the field B . Triplets are common for elements of the second group - zinc, calcium. This is natural: their two outer electrons can be located either on opposite side faces, or on adjacent ones. In the first case, the transverse moments compensate each other (μ_1 is directed along the axis of the core) and the core is established along the field B - a Lorentz triplet is observed. In the second case, the transverse moments are not compensated (μ_1 is directed at an angle θ to the axis) and the atom is rotated at an angle θ to the field B , which leads to splitting as for doublets. As a result, the spectra from two types of atoms are added, and instead of each of the three lines of the triplet, either one, or three, or five is observed, depending on which splitting patterns are added. And in doublets of Group 1 elements, for example, sodium, a single external electron can create a single orientation of the moment μ_1 in an atom, therefore, all lines of the spectrum generate one type of atomic core.

For atoms of groups VI and VII - with 6th and 7th external electrons, for example, chromium, iodine, splitting is even more complicated [7, 8]. It should be borne in mind that an atom in an external field rotates like a drum in the “Field of Wonders” in many ways, depending on how the magnetic moments of the electrons are directed, giving the total moment μ_1 . And these different combinations correspond to different orientations of atoms in space. Thus, each type of atom has its own spectrum, which is easy to check by separating atoms by an inhomogeneous magnetic field and examining their spectra separately [5]. As a result, the atoms that emitted the beam of split lines will decay into beams of atoms, each of which generates its own line or group of lines.

In all cases, the split components are displaced from the central one, as it is believed, by strictly fixed frequency intervals related to the Larmor frequency $eB/4\pi m$ as small rational numbers according to Runge's rule. In fact, exact measurements of the spectra showed that the rule is not strictly followed [7]. The frequencies are slightly different from those calculated from quantum mechanics, as shown by accurate measurements with high spectral resolution instruments, for example, a Fabry-Perot interferometer [9]. After all, $\cos\alpha$ only occasionally coincides with rational numbers (say, for the angles α in Egyptian triangles), for example $\cos 60^\circ = 1/2$. By the way, the sides of the skeleton are inclined to the axis of the bipyramid not necessarily by $\beta = 30^\circ$, but possibly also by 35° , if the skeleton is made of halves of an octahedron - two tetrahedral pyramids, folded not by bases, but by tops. The angle α can be determined by precisely measuring the amount of splitting. In the meantime,

small discrepancies between the splitting value and the calculated one are attributed to inaccuracies in measurements of the field B , Δf and inaccuracies of quantum models.

The splitting model can be verified by forcibly orienting the atomic cores in a given direction. After all, skeletons are usually oriented by the magnetic field at fixed θ and φ , and it is impossible to measure the dependence of Δf on θ and φ . But if the electric field E orientates the core with a dipole moment, and the magnetic B only changes the frequency of generation of electrons at the nodes, then it is possible, by turning the core in different directions and observing the change in the number, polarization and intensity of the components, to check the correctness of the hypothesis. Another way is to observe the Zeeman effect on absorption lines in crystals (for example, xenotime and tizonite [10]). Then the generating atoms, strictly oriented in the crystal lattice, the crystal matrix, will rotate together with the crystal (Fig. 5). By rotating the crystal, one can observe different types of the Zeeman effect, and such an anisotropic Zeeman effect was actually observed in a number of crystals [11], for example, for terbium ions in the aluminate and garnet matrix [12]. Moreover, observing the crystal in a transverse view of the magnetic field from different sides, one can study the dependence of the intensity of the split components on the angles φ , θ and the angle of rotation of the core to the observer, while gas atoms can only observe an averaged pattern. A similar effect is possible in crystals with respect to the electric field: the Stark effect will be found, which depends not only on the atoms of the crystal and the field E , but also on the angles of rotation of the crystal in the field E . And such an anisotropic Stark effect was actually discovered in crystals, confirming the correctness of the model [2, 13]. This resembles the anisotropy of a log: it splits easily in some directions, but not in others. So, you can study in detail the mechanism of the atom, arranged like a tricky Swiss watch or the clock of the Nizhny Novgorod master I. Kulibin in the form of an egg [14]. Kulibin's clock consisted of two halves connected by a jumper, like two halves of an atomic skeleton, with a complex core filling, where hundreds of small wheels were spinning, like electrons, showing the time and revealing a bizarre spectrum of a puppet show. Such mechanisms - the ancestors of modern automatic robots were very popular in Europe of that era, as the example of the Disney cartoon "Pinocchio" shows, where master Dzeppetto (an analogue of Pope Carlo and our Kulibin) built such mechanisms.

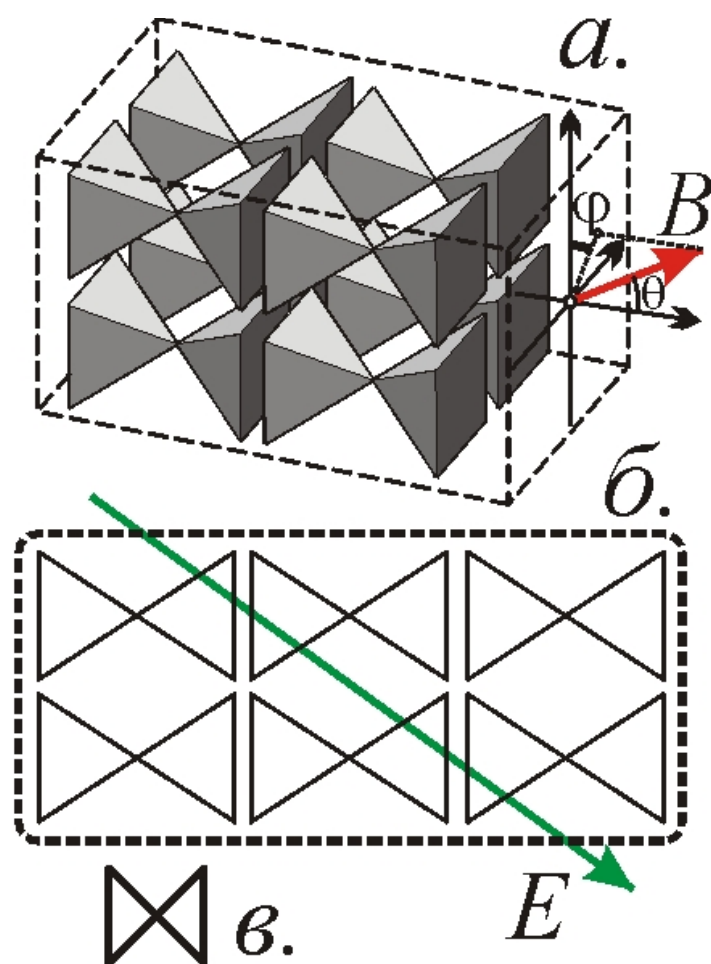


Рис. 5. Кристаллы в магнитном поле B (а) и электрическом E (б). Внизу - скандинавская руна "Дэг" (в).

Fig. 5. Crystals in magnetic field B (a) and electric field E (b). Below - the Scandinavian rune "Dag" (c).

The magnetic model of the atom also explains the effect of paramagnetic resonance - it is caused by electrons located on the bisector of the face, where the intra-atomic magnetic fields B_0 are compensated [5, 15]. If you select two adjacent or two opposite edges of a bipyramid, then a cross is formed that resembles a cross (wagu of puppets) with invisible threads of magnetic field lines extending from it, controlling electrons that spin in a magnetic field and generate radiation. On the bisector of the angle of this cross, the fields B_0 are compensated, but in an external field B , electrons can vibrate with a frequency $f = eB_z / 2\pi m$, and when exposed to radiation of such a frequency f of the microwave range, resonant absorption of radiation occurs. In addition to the external field, the electron is also in the weak field of other electrons and the nucleus, which is specific for different atoms: each atom has

its own individual portrait of the spectrum of resonant frequencies. So, by the method of paramagnetic resonance, the chemical composition of the medium - the atoms included in it - is established.

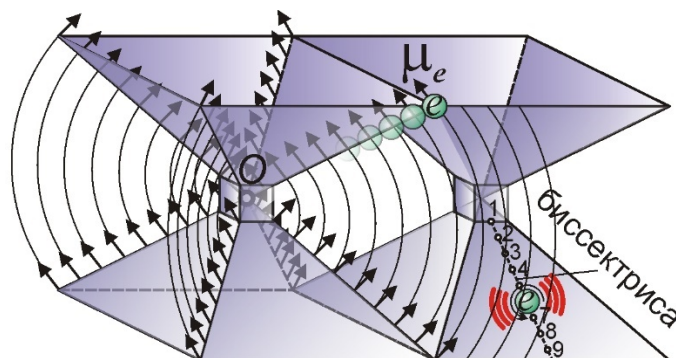


Рис. 6. Формирование молекулярных спектров. Генерирующие атомы располагаются в узлах 1, 2, 3... на биссектрисе грани.

Fig. 6. Formation of molecular spectra. The growing atoms are located at nodes 1, 2, 3... on the bisector of the face.

The spectra of molecules are more complex and become striped, and each band is actually represented by a set of very close lines. Such a spectrum is also generated by electrons on the bisector of the face, which are usually “silent” due to the zero field B_0 , but “wake up” in the field of a neighboring atom (Fig. 6). Since the source of the field is quite distant, in neighboring nodes on the bisector, the magnetic field transverse to the face is small and varies from node to node by approximately the same value ΔB_z . Therefore, the molecular spectrum (called rotational) is almost equidistant, i.e. all lines in the spectrum are separated from each other by almost the same value $\Delta f = e\Delta B_z / 2\pi m$ and are located in the IR range. Light and dark bands of the spectrum alternate, as in a barcode. The value of Δf changes either at distant sites, where the field ΔB_z decreases noticeably, or in other series, where the magnetic field of a neighboring atom is oriented differently from a different location of the neighboring atom. In this case, different atoms with electrons in the same site generate slightly different frequencies, since in addition to the magnetic field of the core, electrons find themselves in the field of neighboring atoms of the molecule, depending on the location of electrons in them, creating slightly different additional fields $B_{mi} \ll B_z$. Therefore, instead of one line $f = eB_z / 2\pi m$, a palisade of lines with frequencies $f_i = e(B_z + B_{mi}) / 2\pi m$ is visible, i.e. a molecular band, the width of which is the greater, the greater the spread of the field B_{mi} - the further the electron is from the center. And precisely, the stripes expand towards the border of the series, i.e. with increasing strip number, node number along the bisector. In solids, when many atoms combine, there are so many lines that they merge into a continuous spectrum, which explains Planck's law of energy distribution in the spectrum of a black body, as the

sum of radiation from nodal electrons, generating fixed frequencies at the nodes, like notes on musical notes lines, and orbiting electrons flying in trajectories, twisting like a treble clef.

The value of Planck's constant h , measured, say, in the photoelectric effect may also be inaccurate. Indeed, depending on the type of atoms, the distances between the dipoles forming the magnetic axes, as well as the directions of the elementary magnetic moments of the charges forming these axes, can change slightly. As a result, the magnetic field changes, in which electrons rotate in orbits around the atom's core and around the nodes on the faces. Indeed, the values of h , measured in the photoeffect or from the Rydberg constant R for hydrogen-like atoms or alkali metal atoms, differ slightly from the tabulated h , and not only from different nuclear masses. And the corrections to R , obtained within the framework of quantum electrodynamics, in the BTR are obtained from different placement of charges in the core - these elementary q .

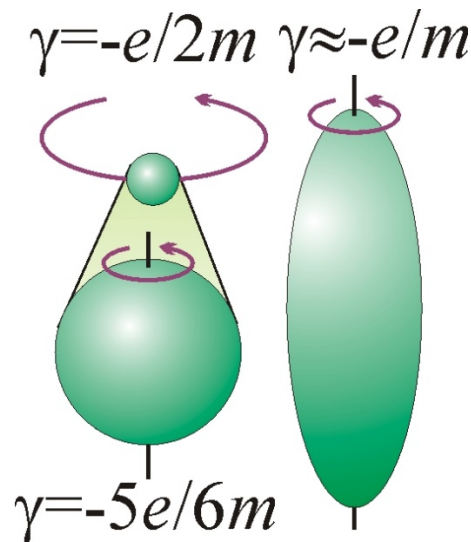


Рис. 7. Гиромагнитное отношение для электрона: Орбитальное (а) и спиновое для шарового (б) и веретёновидного электрона (в).

Fig. 7. Gyromagnetic ratio for an electron: Orbital (a) and spin for ball (b) and spindle-shaped electron (c).

Another anomaly is the gyromagnetic ratio for the electron. As the calculation shows for a charge moving in an orbit, the ratio of the magnetic moment to the angular momentum is always $-e/2m$. But for the spin moment, i.e. the magnetic moment of the electron due to its axial rotation, the gyromagnetic ratio turned out to be twice as large: $\gamma = -e/m$, contrary to the calculations (Fig. 7). Ballistic theory and the magnetic model of the atom solve this puzzle in an elementary way. After all, the

electron emits rheons only from the surface. And since the emission of rheons leads to the appearance of an electric effect of the charge, this charge is distributed over the surface, and the mass of the electron is distributed throughout the entire volume. As a result, for an electron in the form of a ball, the angular momentum is $N=2mr^2\omega/5$, and the magnetic moment when integrating over the sphere is $\mu=-e\omega r^2/3$. Hence, the gyromagnetic ratio $\gamma=\mu/N=-e5/6m$, which is already close to the measured gyromagnetic ratio for an electron. If the electron has the shape of an ellipsoid elongated along the axis of rotation, then the ratio can become arbitrarily close to $\gamma = -e/m$. Moreover, a small difference of the coefficient in γ before e/m from unity downwards is actually observed in the experiments of Barnett and Einstein-de Haas [16]. Note that at the beginning of the last century, some scientists, for example Abraham, found the calculated value $\gamma=-e5/6m$ from the representation of an electron as a ball, if its mass is of an electromagnetic nature - a hypothesis studied in detail by Ritz. Due to the difference in the shape of the electron from the ball, its magnetic moment differs from the Bohr magneton $\mu_H=e\hbar/2m$: $\mu\approx 1,00012\cdot\mu_H$. This difference is difficult to express in quantum electrodynamics in terms of the fine structure constant α . And in the classical magnetic model of the atom and the electron, this is a difference and the value of α itself is simply a consequence of the nonsphericity of the electron (α will be expressed through the ratio of the electron semiaxes).

A correct understanding of the nature of the magnetic field of an atom is also key to understanding the magnetic and superconducting properties of materials. Earlier, it was noted that elements of even periods, in which the filling of the layer with electrons along the perimeter of the upper part of the bipyramidal skeleton resembling a cap with a tassel, should have magnetic properties [15, 17]. Let us recall that electrons gradually fill the level along a coiling square spiral, such as an antenna in magnetic cards that serve as a key-pass in the subway. Electrons alternately fill the entire upper layer, then the lower one, then the upper layer again, etc., in order to minimize the energy of interaction with the positive nucleus in the center of the core, and with the magnetic field of the core. It is in relation to the direction of its magnetic field that we can talk about the top or bottom. In this way, the magnetic model predicted ferromagnetism even for those elements for which magnetism was not expected [3]. On the other hand, based on the properties of the periodic table, we can assume similar properties for elements of odd periods of the same groups (Si, P, S, Mo, Ru, Rh, Pd, actinides). Indeed, ferromagnetism or antiferromagnetism has been found in a number of such elements, for example, in actinides, including uranium, neptunium, plutonium, etc. [18]. Specific magnetic properties can be expected, for example, for sulfur compounds.

Since magnetism and superconductivity are related phenomena [3], superconducting properties of these elements can also be assumed [17]. Indeed, many

lanthanides are not only ferromagnets, but also superconductors [19]. And actinides - thorium, protactinium, uranium and a number of Th, Pa, U compounds turned out to be superconductors [4, 19]. Superconductivity can also be expected in plutonium compounds. Such high-temperature superconductors are very much needed in electronics and robotics, because they allow you to create simple switch-relays (keys on the Josephson contact). Indeed, it is on cryoelectronic circuits from cryotrons that it is proposed to build artificial intelligence devices, as in the stories of A. Azimov and A. Clark [20]. On the basis of a nonlinear magnetic connection, a domain structure with memory, it is also possible to create new types of thinking machines - where the processes are not digital, but analog, as in the neurons of the brain and the film "Short Circuit". Whether a magnetic conscience will also appear in such machines is a question, but they will be able to think and learn by themselves. Superconductor-magnet combinations will become the basis for robots, parts of which are remotely held and moved like in puppets, but the role of invisible threads is played by the magnetic field lines and radio waves for transmitting commands [17], and the role of the control cross (wag) is played by a microcircuit with branches of leads. Surely, there are substances that go into a superconducting state under normal conditions, at room temperature, which can explain the ancient soaring statues and flying vehicles on superconductors hovering in a magnetic field [17], as in the film "Journey to the Center of the Earth". However, all this precious ancient knowledge, together with the model of the structure of the atom, the superconducting properties of ferromagnets and antiferromagnets, have sunk into oblivion, sank under water with Atlantis [21], like an island in Jules Verne's story "The Adventures of Uncle Antifer", or got lost in the snows of the mountains, as Obruchevskaya "Sannikov Land" and "Plutonium".

But back to the discussion of the well-known candidates for superconductors and ferromagnets. Take the same plutonium: its use as a magnetic and superconducting material is especially promising, because plutonium has six crystalline modifications and six oxidation states [20], ie it forms a wide range of crystals and compounds with unique properties. Although plutonium itself has not yet been found to have superconductivity, a number of its compounds turned out to be superconductors with a critical temperature T_c an order of magnitude higher than that of compounds of similar elements. And they are trying to create a new class of superconductors based on plutonium. In a way, these accidentally discovered "magic" substances - high-temperature superconductors, which at $T_c > 20^\circ \text{C}$ will allow the creation of new types of robots, similar to the animating powder from the fairy tale of A.M. Volkova "Urfin Deuce and His Wooden Soldiers" (she also had a Western prototype - LF Baum's fairy tale "The Land of Oz" and the Russian fairy tale "The Flying Ship [Летучий корабль](#)", where "firewood" revived "battle droids" [22]). And in Volkov's tales, they built "battle droids" due to the properties of the new substance.

By the way, this tale of a four-sector country is also saturated with the symbolism of a crystalline pyramidal tetrahedral atom, with a yellow sodium line as a key [21].

So, the magnetic model of the atom has tremendous predictive power. The splitting of spectral lines in the Zeeman effect, opening the way to the structure of the atom, also opens up ways of nuclear fission. Indeed, the Zeeman effect is caused not only by the external magnetic field, but also by the field of the nucleus. This is revealed by the Mössbauer effect, which makes it possible to study the fine structure of X-ray and gamma spectra. The Mössbauer effect itself is also associated with magnetism. For example, the core of cobalt Co transforms into an iron core Fe when an electron is captured from the K-shell of the atom, where the electron has a strictly fixed energy. Therefore, when accelerated by the core, rotating in the magnetic field B_0 of the core, it emits at a fixed frequency, which is maintained with an accuracy of 10^{-12} . Neighboring atoms, for example, in a hematite crystal (Fe_2O_3) slightly change the electron energy and the field B , and in a number of ways, depending on the location of the core. As a result, the Mössbauer absorption line also splits [23]. It is not excluded that the fission of the plutonium nucleus can be accomplished by controlling the internal and external magnetic fields that affect the structure of the nucleus and its stability. So, it is the magnetic bipyramidal model of the atom and the nucleus that explains why heavy nuclei are divided into parts whose mass ratio is close to the golden ratio - the Phidias number - $\Phi = 1.618$ [24] - this is the ratio of the masses of two pyramids of the nucleus, ie neighboring magic numbers [15, 21]. No wonder the number Φ had a magical, sacred meaning.

Note that it is mainly with the help of a magnetic field that they penetrate the secrets of the microworld, because magnets are used in devices for extracting the radiation energy of an atom, for example, in masers. Masers of natural origin have also been found in space. For example, around the stars of the Mira type (Omicron Ceti - Mira), there is a region emitting intense radio lines of gas, just like terrestrial masers. This area forms a ring around the star. Indeed, according to the Ritz effect, the light of the central star is usually re-emitted by gas located within the plane of the ellipsoid section, i.e. just within the ring [22].

The most interesting thing is the observation of the Zeeman effect in the spectra of stars. It is assumed that the doubling of lines and strong polarization of radiation in the spectrum of polars and magnetic stars, as well as white dwarfs, is associated with the Zeeman effect, for example, in the star EUVE J0317-855. But rather, the polarization is caused by the movement of the stars - the blurring of their images and electronic orbits. Therefore, for example, in β Lyra, the polarization changes synchronously with the orbital motion and the change in the apparent shape of the stars. Of course, stars have magnetic fields, but small, on the order of those found in the Sun. In distant stars, due to the acceleration from the Lorentz force in

these fields, there is a strong shift of the radiation frequency alternately up and down. This leads to a symmetric broadening of the lines of white dwarfs, a number of red dwarfs and supergiants [25]. If the broadening occurred only due to the dispersion of radial accelerations on the stellar surface, it would turn out to be asymmetric - only in the red side, contrary to observations. This effect was also found in galaxies in the redshift range $0 < Z < 2$ [26], in emission lines, for which the Ritz effect is especially large, since they are almost not re-emitted by the medium. That the reason for the Ritz effect is confirmed by the increase in the line width in proportion to the redshift Z , i.e. distance r . The effect is especially pronounced for quasars and Seyfert galaxies, for which the width of the emission lines is $\Delta\lambda \sim (0.01-0.1)\lambda$; is close to their displacement $\Delta\lambda \sim Z\lambda$ [27].

Likewise, variable polarization, anomalous properties of magnetars, pulsars and sources of gamma-ray bursts (GRBs) are apparently associated not with the magnetism of these stars, but with the Ritz effect, which causes illusory flares in the gamma range and variations in their period. Thus, near the source in the constellation Pisces, which flared up in 1979 [26], the brightness pulsations were obviously caused by the orbital rotation of the star. Therefore, in accordance with Ritz's theory, a sharp outburst was observed, followed by a smooth extinction with oscillations of a variable period [28].

But the main keyhole that hides all the secrets of space is in the core, or rather in the core, in the center of the Galaxy - in the radio-emitting object Sgr A*, where the supermassive black hole is believed to be. It is believed that its gravity, like a powerful magnet, leads to rapid motions of stars near the center of the Galaxy (Fig. 8). Moreover, the giant speeds of stars are established both by the apparent motion and by the spectra, which fully correspond to the observed motion of the stars [29]. But other explanations for the rapid motions in the center of the Galaxy can also be considered. Moreover, the absence of supermassive bodies in the center of our and other galaxies confirms the emission spectrum of these areas, which corresponds to an extremely rarefied gas, judging by the presence of forbidden lines in the spectrum [7, p. 374]. A supermassive black hole would cause accretion of interstellar gas, an increase in its concentration and temperature. In addition, it would lead to a fast precession, a rotation of the orbits of the stars faster than that of Mercury. But no such effects were found.

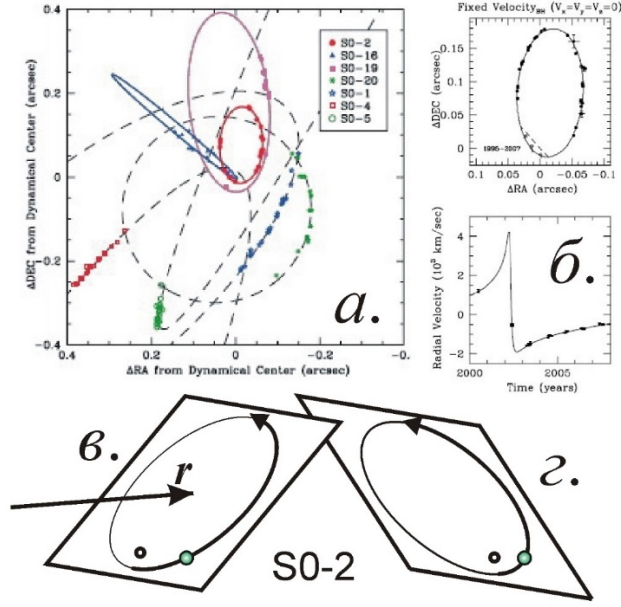


Рис. 8. Движение звёзд возле центра Галактики Sgr A* (а), орбита и кривая лучевых скоростей (б) звезды S0-2. Два астрометрически неразличимых варианта расположения орбиты звезды (в, г).

Fig. 8. Movement of stars near the center of the Galaxy Sgr A* (a), orbit and radial velocity curve (b) stars S0-2. Two astrometrically indistinguishable variant of the location of the star's orbit (c, d).

Therefore, it is more natural to assume that there is an illusory increase in the speed of the apparent motion of stars due to their motion with an acceleration close to the critical one $a_c \approx -a_0 = -c^2/r$. For example, if a star system with a massive central star moves with a radial acceleration $-a_0$ in the gravitational field of another massive star or star cluster. Let's take a trip to the center of the Galaxy and calculate how many times the apparent motion of a star is accelerated if $(1 + ra_c/c^2) = b < 1$, i.e. the compression ratio g , showing how many times the apparent motion is accelerated compared to the true one, will be equal to $g = dt/dt' = 1/b > 1$. In the case of the closest approach of acceleration to critical $-a_0$, a frequency overmodulation (FFM) regime will arise, when small modulations of the speed of light with $c' = c - V_r$, caused by proper motions of stars with a radial velocity V_r , will cause giant frequency variations. In the general case, the period of light oscillations is transformed as

$$T' = \left(1 + \frac{V_r}{c'} + \frac{ra_r}{c'^2}\right) T = \left(1 + \frac{V_r}{c'} + \frac{b-1}{(1-V_r/c)^2}\right) T \approx \left(b + \frac{V_r}{c} - 2\frac{V_r}{c}\right) T = \left(1 - \frac{V_r}{cb}\right) bT \quad (1)$$

Thus, the motion of the stars looks accelerated by a factor of $g = 1/b$ times, so that the measured astrometrically transverse speed of the stars is $V_t'(t) = V_t T/T' = V_t(t)/b$. And the radial velocity, measured spectroscopically, if we study the relative

displacements of the lines from their mean positions, will be $V_r'(t) = -V_r(t)/b$. Thus, in both cases, there is an illusory increase in the speed by a factor of g , but in the second case, the calculated direction of the speed becomes reverse. It would seem that this would lead to a discrepancy between the observed astrometrically motion and the measured spectroscopically. In fact, from the uncertainty of the angle $i=i_0$ of the orbital inclination, since only the projection of the orbit and apparent motion onto the plane of the sky is observed (Fig. 8), they can correspond to two indistinguishable variants of the orbital position $i=i_0$ and $i=-i_0$. And each position of the star will correspond to two possible values of the radial velocity $V_r'=V_{r0}$ and $V_r'=-V_{r0}$. Thus, in the orbital elements, determined astrometrically and spectroscopically, there are no contradictions, but instead of the true angle $i=i_0$, a false value $i=-i_0$ will be obtained, which corresponds to the radial velocity $V_r'=-V_{r0}$.

The discrepancy can be identified by the spectrum of the star, in which it is possible to clearly distinguish the absorption and emission spectrum of interstellar gas [27]. If for a true orbit with $i=i_0$ the most distant point corresponds to the most intense absorption spectrum of interstellar gas, for a false orbit with $i=-i_0$ the closest position of the star and a weak absorption spectrum of gas correspond to the same motion of the star on the plane of the sky, which will mean an incorrect value i and radial velocity sign inversion. And if you measure not by the relative shift of the spectral lines, but by the absolute one, you can also find a discrepancy, because from formula (1) at $T' \ll T$ by the Doppler effect, the radial velocity $V_r' \sim c$ is required. So, there is a huge shift of the spectral lines, which is not noticed because the spectral lines are incorrectly identified. Apparently, the recorded spectral lines of helium and bromine actually correspond to the low-frequency radiation of the far-IR and radio lines of hydrogen and helium, shifted by the Ritz effect to the near-IR range.

If the astrometrically and spectroscopically measured motions of stars near the galactic center are illusory accelerated by the Ritz effect by a factor of $g=1/b \sim 400$ times, then the true velocities will turn out to be much less, and the orbital periods are much greater than the calculated ones. For example, for the star S0-2, instead of the measured speed $V_r' \sim 4,000$ km / s, we find that the true speed is $V_r \sim 10$ km / s, and the orbital period is not $P'=15$ years, but $P=6,000$ years. Then the mass of the central star is not $M' \sim 4 \cdot 10^6 M_\odot$, but $M=M'/g^2 \sim 25 M_\odot$, i.e. a magnitude typical of O and B main sequence stars. In this case, the characteristic masses of satellite stars will be $\sim 0.1 M_\odot$. For a star system to move during such a time $P \sim 6,000$ years with an acceleration close to the critical $a_c \sim -a_0 = -c^2/r$, it must fly in the gravitational field of a globular cluster located at a distance of $R \sim 100,000$ AU from the star. and having a mass $M \sim 10^7 M_\odot$. Such a system can include 10^6 stars with a mass of $\sim 10 M_\odot$. In this case, a globular cluster can have a size of $\sim 10,000$ AU, leading to the motion of the central star with a period of $P \sim 10,000$ years.

Such massive clusters are just typical for the center of the Galaxy, in the core, where the concentration of stars is maximum. And the center itself serves as the center of gravity, capable of providing a critical acceleration $a_c \approx -a_0$. Indeed, according to the known mass distribution [25, p. 197], inside a sphere of radius R near the center (in the core) of the Galaxy $m(R)=kR$, where $k=10^7 M_\odot \text{ 1 / pc}$. Hence, the critical distance R_c is found from the condition that the acceleration on the surface of the ball is equal to the critical one $a_0=Gm/R_c^2$. Whence $R_c=Gkr/c^2=1.5 \cdot 10^{14} \text{ m}=1,000 \text{ AU}$. This R_c value within the order of magnitude corresponds to the sizes of the orbits of S0-2 and other stars moving around the central object [29]. Thus, within a sphere of radius $R_c=1,000 \text{ AU}$. in the center of the Galaxy, many objects flying around the center have an acceleration of the order of critical. Hence - the activity arising from the Ritz effect, flares, rapid movements, ionizing radiation in the center of our and other galaxies. So relativistic astronomers turned the center of the Galaxy into a Field of Wonders in the Land of Fools, where millions of solar masses “grow” from one star. In fact, all phenomena can be explained by the classical motion of an ordinary star system in an orbit around the center of the Galaxy or another star system.

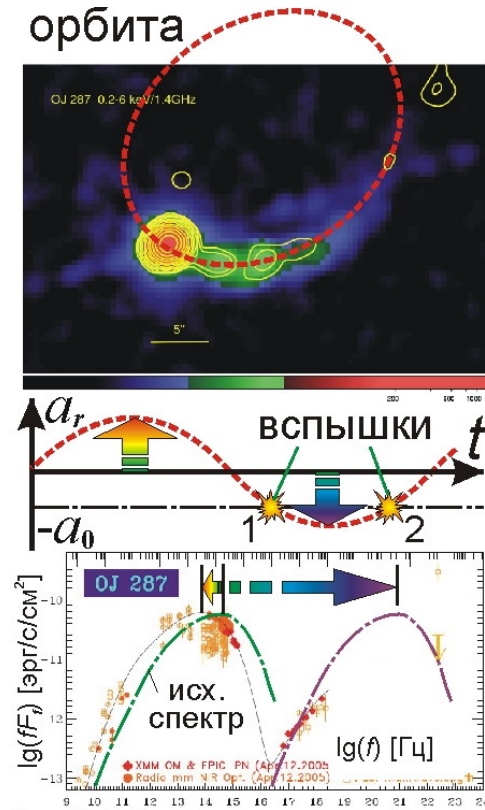


Рис. 9. Орбитальное движение блазара OJ 287 ведёт к размытию изображения и вспышкам. Ниже - график ускорений и спектр блазара за счёт Ритц-эффекта.

Fig. 9. Orbital motion of the blazar OJ 287 leads to image blur and outbreaks. Below is a graph of accelerations and the spectrum of the blazar due to the Ritz effect.

The blazar OJ 287 was also considered such a double supermassive black hole, which explained its flares when one hole crossed the accretion disk by another. But it can also be two simple stellar systems that change brightness according to the Ritz effect when moving in orbit. This orbit is even visible: along it the blazar image is blurred (Fig. 9) and is split into three - such a multiplication of images in electrodynamics was also predicted by Ritz. Moreover, orbiting with a period of 12 years leads to a typical flare twice per period. Interestingly, astrophysicists obtain similar light curves based on the beaming effect - the brightness-changing relativistic Doppler effect in plasma jets moving at high speed [30], like a beard developing away from a rotating star [21, 22, 28]. The superluminal speeds of OJ 287 and its jets are also a consequence of the acceleration of visible processes by the Ritz effect. It is not for nothing that OJ 287 is called the Rosette stone of astrophysicists [31]: it is this blazar that sheds light on the hieroglyphs of the blazar spectra. The spectrum of all blazars contains two distinct maxima - in the visible range and in the X-ray range. Within the framework of the Ritz effect, their origin is obvious: the stars in the blazar system move in orbits with an acceleration close to the critical one, and for a significant part of the orbital period their acceleration is maximum $a_r \approx a_0 = c^2/r$ or minimum $a_r \approx -a_0$. Accordingly, for some of the stars the radiation frequency is reduced by about two times ($f' = f/2$), while for the other part it is increased by about a thousand times according to the Ritz effect $f' = f/(1 + a_r/a_0) \gg f$. The resulting blazar spectrum is the sum of two spectra - the usual thermal one, but with half the color temperature of the stars, and the X-ray one - repeating the optical one, but shifted into the X-ray range (Fig. 9). And exactly, the spectrum is represented by the sum of two spectra, close to thermal, and their maxima are approximately equal, since the radiation time of stars in both positions is approximately equal. So, the fabulous objects (such as neutron stars, etc.) from fabulous matter the Ritz effect magically turns into ordinary stars, although the effect itself gave rise to the illusion of the activity of these objects.

Thus, modern tales of dark matter and supermassive black holes, etc. sometimes even more fantastic than the previous myths about the world floating in the ocean on the back of a giant turtle with four elephants on its shell, as figuratively shown in the film "The Color of Magic". Previous ideas will be even less fantastic if by the ocean we mean space, by the universal disk and the turtle - the Earth or the galaxy, and under the four elephants - the foundation of the universe, an atom with its four faces, on which electrons live. On one ancient engraving there is an image of a man who, on the advice of G. Bruno, punches a hole in the dome of the firmament at the edge of the world and sees behind it a completely different picture of phenomena - the seamy side of an illusory puppet show playing out in the firmament. So, the BTR, breaking through the light barrier and crystal spheres of the atom, reveals the true causes of the phenomena, allowing you to see the phenomena in their true light. Perhaps it was G. Bruno who became the prototype for the image of Buratino by L.N.

Tolstoy, because just like “Pinocchio” Collodi was born and lived in Italy, wandered around the world, sowing revolutionary ideas, trying to free people from dogmas, by the way, like Collodi himself, a participant in the national liberation movement. And Pinocchio almost shared the part of Bruno, who was burned at the stake. And the role of the Inquisition, of course, was played by Karabas-Barabas with his whip and fire. For Collodi himself, the prototype of Pinocchio, apparently, was Cyrano de Bergerac - a nosed poet who wrote a lot in the style of burlesque [22] and recklessly stabbed with a sharp word and sword.

The key to rethinking the microworld and megaworld (space) is the magnetic model of the atom, harmonious like a clock or a lyre. It is not for nothing that the atom has long been compared with a musical instrument, organ, barrel organ, musical snuffbox [6, p. 102]. According to the myth, Orpheus just with the help of the lyre descended into the underworld and traveled there, like an atomic underground boat from the movie "The Core". So, the lyre played the role of the key to this world. It is possible that the mythical representation of Hades (Greek hell) is a symbolic image of the microworld (atom, hence the consonance) or megaworld (the nucleus of the Galaxy), and the lyre is an ancient model, the symbol of the atom. And in the biblical myth, considered, for example, by Dante, hell (as well as heaven) consisted of 7 levels (circles) [32], which corresponds to 7 levels of the atom, on which electrons are located (hence the 7 periods of the periodic table). Similarly, in Greek myths, the underground kingdom is multi-storey - Tartarus was located under Hades. And in Russian fairy tales, under the copper (or iron) one there was a silver kingdom, and under it - a golden one. Just like the elements Cu, Ag, Au are located in the long-period periodic table one below the other in periods corresponding to the filling of the levels-levels of the atomic core with electrons. By the way, in the Russian fairy tale Sadko traveled in the underwater kingdom like an atomic submarine thanks to the harp, which could also symbolize the atomic model [7]. It turns out that the ancient idea of hell is just a stylized idea of the microcosm of eternal chaos, atomic fire, and nuclear reactions. As well as the micro-door located behind the hearth in the tales of Buratino or Alice L. Carroll [28]. To open and pass through this door, it was required to decrease, change for a short time the atomic structure. Knowledge of the structure of the atom will just make it possible to build such underground boats, penetrating through rocks, as in the story of G. Harrison "Penetrated into the rocks [Проникший в скалы](#)". After all, atoms are almost 100% empty space, where the nucleus and electrons account for a tiny fraction of the volume, therefore, by swinging electrons, atomic skeletons by an external field, you can “squeeze” solid bodies through the rock [3]. Probably, such a symbolic description of the microworld also exists in the matrix version of quantum mechanics. The matrix just resembles an atomic plane in structure, where numbers are located in cells, nodes. And the microcosm is similar to the world of the film “The Matrix” - the digital world of magnetic memory matrices,

where the values of coordinates, moments change discretely, according to strict rules, as in programs, the first of which were developed by Ada Lovelace (Byron) just in the years when spectroscopy appeared.

The symbolism of the atom is also found in folk crafts. Patterns on Russian shirts, accordions, etc. of rhombuses and opposing triangles very much resemble the pixel structure of an atom. Similarly, in games such as tic-tac-toe, renju, dots originating from ancient games, such as chess and go, the discrete structure of an atom with nodes in which particles of two types can be located and jump can be reflected - negative electrons or positive nuclei and positrons forming complex configurations [15, 33]. The perfection, grace of the clockwork of the atom and the arrangement of microparticles are so amazing that they create the illusion that they, like the model of the atom itself, were constructed at the beginning of time by some skillful craftsman like Kulibin. The reflection of this model of the atom can be seen in the Scandinavian runes, for example, in the “Dag” rune, which just means “light”, “middle of the day, summer,” because the atom is an elementary emitter of light, the center, the basis of the universe. It is no coincidence that the rune “Dag” is the last one, located at the bottom of the alphabet: so, atoms, nuclei lie in the foundation of the universe. So it is not in vain that the runes serve as the key to the basement floors of the universe in the novels of Jules-Verne and R. Tolkien. By the way, the first letter of the Russian alphabet "А" could originally mean the basis of the world - an atom (remember E [5]), and the last letter of the Cyrillic alphabet "И", which resembles in the ancient spelling (in the initial letter - "Izha" æ [34]) a rune “Dag” could symbolize the core [28]. The letters could also symbolize individual elements, especially since the dots in many letters (e, i) resemble Langmuir's designations for electrons at the atomic core. And the very ancient Slavic alphabet-initial 7×7 [34] and the Sanskrit alphabet resemble the periodic table, in which the elements are designated by letters (in the original alphabets the number of letters reached 100, as in the table - elements). The scientist originally constructed the table - as a 7×7 matrix. Moreover, the alphabet is a universal matrix, such as a magic square, which gives the key to both the microworld and the cosmos [33, 34, 35], hence the alchemical correspondences of elements and planets. Therefore, the alphabet, originally received by Buratino from Pope Carlo, was in itself the key to the universe, if only he knew. As such an alphabet “with wonderful color pictures” and a key - a symbolic image of the structure of electrons, atoms, protons, microworld and space, the astrobook by I. Levitt can also act [36]. The model of the atom and the nucleus can be seen in the Egyptian pyramids [5, 37], and even in the symbols from the cover and disk of the journal "Chemistry and Life" (it is just devoted to the analysis of the properties of atoms and compounds). And the editorial office of the journal is located in Moscow in the building of the Institute of Egyptology, among the buildings of chemical institutes.

Thus, the ballistic theory and the magnetic model of the atom reveal not only the secrets of the structure of the atom and space objects, but also allow us to understand the structure of elementary particles, including for the release of the giant energy hidden in them, as described in more detail in the author's reports at the International Conference [38] and scientific and technical mini-conferences [39, 40]. So, it is the ballistic theory and the magnetic model of the atom that bring liberation from the web of dogmas imposed by puppeteers who manipulate the minds of their puppets. And the magnetic model of the atom serves as the magnetic key that opens the way to the freedom of thought, science and the release of the energy of the microworld - the atomic hearth, behind which the door of the atomic nucleus is hidden.

Semikov S.A.

Sources

1. Tolstoy L.N. Fairy tales. Kiev: BMP "Borisfen", 1995.
2. Seisyan R.P. // Window to the microcosm. 2006. Issue. 2 (6).
3. Semikov S.A. Temperature anomalies and crystalline cryotechnology // Engineer. 2016. No. 5. [[Семиков С.А. Температурные аномалии и кристаллические криотехнологии // Инженер. 2016. №5.](#)]
4. Mineev V.P. Superconductivity in uranium ferromagnets // Phys. 2017. No. 4.
5. Semikov S.A. Atomic magnet and the spectral code of the atom // Engineer. 2015. No. 5-6. [[Семиков С.А. Атомный магнит и спектральный код атома // Инженер. 2015. №5–6.](#)]
6. Seabrook W. Robert Wood. Moscow: Nauka, 1980.
7. Frisch S.E. Optical spectra of atoms. M.-L.: Fizmatgiz, 1963.
8. Cheplashkin V.M. Spectral Line Splitting in a Magnetic Field // Galilean Electrodynamics. 2017.
9. Vdovin V.A., Zakharov Yu.N. Zeeman effect. N. Novgorod: UNN, 2014.
10. Landsberg G.S. Optics. Moscow: Nauka, 1976. [[Ландсберг Г.С. Оптика. М.: Наука, 1976.](#)]

11. Golubev V.G. et al. // FTP. 1987. Vol. 21. S. 30.
12. Kolmakova N.P. et al. // Solid State Physics. 1990. T. 32. No. 5. S. 1406.
13. Alekseev P.S. // ZhETF. 2015. T. 148. V. 3. No. 9.
14. Kochin N. Kulibin. Gorky, 1985.
15. Semikov S.A. From Atom to Nucleus // Engineer. 2007. No. 12. [[Семиков С.А. От Атома до Ядра // Инженер. 2007. №12.](#)]
16. Barnett A. // Phys. 1937. T. 18. No. 7. P. 392.
17. Semikov S.A. Stubborn riddle of magnetism // Engineer. 2012. No. 11–12. [[Семиков С.А. Упрямая загадка магнетизма // Инженер. 2012. №11–12.](#)]
18. Belov K.P., Bochkarev N.G. Magnetism on Earth and in Space. Moscow: Nauka, 1983.
19. Ivanov V.A. And superconductivity and superconductors. M.: Knowledge, 1991.
20. Popular library of chemical elements. Moscow: Nauka, 1983.
21. Semikov S.A. BTR and a picture of the universe. N. Novgorod: Perspective, 2013. [[Семиков С.А. БТР и картина мироздания. Н. Новгород: Перспектива, 2013.](#)]
22. Semikov S.A. Magnetic stars - the compass of a starship // Engineer. 2017. [[Семиков С.А. Магнитные звёзды – компас звездолёта // Инженер. 2017.](#)]
23. Sivukhin D.V. Atomic and Nuclear Physics. Part 2. M.: Science. 1989.
24. The world of mathematics. T. 1. Korbalan F. Golden section. M.: De Agostini, 2014.
25. Physics of space. Moscow: Soviet Encyclopedia, 1986.
26. Thomas D., Steele O., Maraston C. et al. // MNRAS. 2013. V. 431. P. 1383.
27. Daukurt G. What are quasars? Kiev: Radianska school, 1985. [[Даукурт Г. Что такое квазары? Киев: Радянська школа, 1985.](#)]

28. Semikov S.A. Cosmic metamorphoses of time // Engineer. 2016. No. 8-9. [[Семиков С.А. Космические метаморфозы времени // Инженер. 2016. №8–9.](#)]
29. Ghez A. M., Duchene G., Matthews K. et al. // Astroph. J. 2003. V. 586. L127.
30. Villata M., Raiteri C. M., Sillanpaa A. et al. // MNRAS. 1998. V. 293. [[Villata M., Raiteri C.M., Sillanpaa A. et al. // MNRAS. 1998. V. 293.](#)]
31. Takalo L.O. OJ 287: The Rosetta stone of blazars // Vist. Astron. 1994. V. 38. Is. 1.p. 77.
32. V. V. Evsyukov. Myths about the universe. М.: Politizdat, 1986. [[Евсюков В.В. Мифы о мироздании. М.: Политиздат, 1986.](#)]
33. Semikov S.A. Geometry is the key to the microworld // Engineer. 2008. No. 2. [[Семиков С.А. Геометрия – ключ к микромиру // Инженер. 2008. №2.](#)]
34. Semikov S.A. Alphabet brought from the stars // Engineer. 2011. No. 4. [[Семиков С.А. Алфавит, принесённый со звёзд // Инженер. 2011. №4.](#)]
35. Semikov S.A. Key to the mysteries of space // Engineer. 2006. No. 3. [[Семиков С.А. Ключ к загадкам космоса // Инженер. 2006. №3.](#)]
36. Levitt I. Beyond the Known World: From White Dwarfs to Quasars. М.: Mir, 1978. [[Левитт И. За пределами известного мира: от белых карликов до квазаров. М.: Мир, 1978.](#)]
37. Semikov S.A. Atomic crystal pyramid // Engineer. 2009. No. 3. [[Семиков С.А. Атомный кристалл-пирамида // Инженер. 2009. №3.](#)]
38. Semikov S.A. Magnetic model of the atom and its application in microelectronics // Sb. Proceedings of the II Russian-Belarusian Conference “Element Base of Domestic Electronics” November 17-19, 2015 N. Novgorod, 2015. P. 420. [[Семиков С.А. Магнитная модель атома и её применение в микроэлектронике // Сб. трудов II российско-белорусской конференции “Элементная база отечественной электроники” 17–19 ноября 2015 г. Н. Новгород, 2015. С. 420.](#)]
39. Semikov S.A. Strong interactions and armored personnel carriers // 38th Scientific and futurological readings of NTORES. UNN, October 29, 2014

[[Семиков С.А. Сильные взаимодействия и БТР // 38-е Научно-футурологические чтения НТОРЭС. ННГУ, 29 октября 2014 г.](#)] URL: www.rf.unn.ru/eledep/confesem.npo_popova

40. Semikov S.A. Active regions of galaxies as manifestations of the Ritz effect // 68th Scientific and Technical Miniconference-Seminar NTORES. UNN, October 18, 2016 [[Семиков С.А. Активные области галактик как проявления эффекта Ритца // 68-я Научно-техническая миниконференция-семинар НТОРЭС. ННГУ, 18 октября 2016 г.](#)] URL: [http://www.rf.unn.ru/eledep/confesem.npo_popova/2016_10_18\(68\)/03.pdf](http://www.rf.unn.ru/eledep/confesem.npo_popova/2016_10_18(68)/03.pdf)

Installation date: 02/07/2017



Russian to English translation using Google Translate by Thomas E Miles. Original Russian language files located at: <http://www.ritz-btr.narod.ru/>. Other Ritz related files located at the Robert Fritzius web site: <http://shadetreephysics.com/>